Wall Slip in the Capillary Flow of Molten Polymers Subject to Viscous Heating

Eugene E. Rosenbaum and Savvas G. Hatzikiriakos
Dept. of Chemical Engineering, University of British Columbia, Vancouver, B.C., V6T 1Z4 Canada

The traditional way of determining the slip velocity of molten polymers is the classic Mooney technique, which utilizes experimental data obtained from a capillary rheometer. However, measurements of the rheological properties of polymer melts in capillary flow at high shear rates are often complicated by viscous heating, which is not taken into account by this method. A data analysis procedure based on a mathematical model for nonisothermal capillary flow of molten polymers is developed. Conduction, convection, and viscous heating are included, together with the effect of wall slip. The technique provides detailed velocity and temperature fields in the die, and can be used to determine the slip velocity at high shear rates corrected for the effect of viscous heating. It is tested for the capillary flow of several polymers, including polystyrene, polypropylene, high-density, and linear low-density polyethylenes.

Introduction

It is generally accepted that polymer melts, unlike Newtonian fluids, may violate the classic no-slip boundary condition of Newtonian fluid mechanics and slip over solid surfaces when the wall shear stress exceeds a critical value (Ramamurthy, 1986; Kalika and Denn, 1987; Hatzikiriakos and Dealy, 1991). In several polymer processes, the melts are subject to very large shear stresses that often exceed this critical value (usually about 0.1 MPa). To simulate these processes realistically, a reliable slip velocity model is needed that adequately describes the interfacial behavior of polymer melts.

It is also well known that whenever a viscous material is deformed in a flow field, some of the work of deformation is converted into thermal energy by means of viscous dissipation (Winter, 1977; Cox and Macosko, 1974). This phenomenon, generally known as viscous heating, is typical in the processing of molten polymers. Most polymers have high viscosities and low thermal conductivities, which in combination with large process shear rates can lead to a significant increase in temperature.

One of the common tools used to study the rheological behavior of molten polymers, as well as the wall-slip phenomenon, is the capillary rheometer. The traditional way of detecting and quantifying the presence of wall slip is to use experimental data from a capillary rheometer and the classic Mooney method (Mooney, 1931). This technique requires the performance of capillary experiments with a series of dies with the same length-to-diameter ratio, L/D, in order to keep constant the effect of pressure and different diameters, D. If slip occurs, the flow curves (wall shear stress vs. apparent shear rate) start diverging (become diameter-dependent) at a certain value of wall shear stress. This value is taken to be the critical shear stress for the onset of slip. The Mooney method has been used for a variety of polymers by several authors in the past to determine their slip velocity as a function of the wall shear stress (Lupton and Regester, 1965; Blyler and Hart, 1970; Ramamurthy, 1986; Hatzikiriakos and Dealy, 1992).

One of the basic assumptions of the Mooney method is neglecting the temperature and pressure effects. However, it is reasonable to expect that the effect of viscous heating is quite significant at sufficiently high shear rates, at least for some types of polymers. Thus, one can expect that the Mooney method cannot be applied in all cases. Indeed, many researchers pointed out that experimental data points on the Mooney plot (apparent shear rate vs. inverse of capillary diameter) do not fall on a straight line as this technique presumes (Lupton and Regester, 1965; Shih, 1979; Hatzikiriakos et al., 1995). Instead, the data define curves exhibiting a tendency to bend toward the higher apparent shear rates with increase in the die diameter (convex downwards). Usually such anomalies are ignored by researchers in the field, which may lead to inaccurate slip-velocity calculations.

Correspondence concerning this article should be addressed to S. G. Hatzikiriakos.

Viscous heating in the capillary extrusion of polymer melts has been the subject of several reviews and studies over the past decades (Winter, 1977; Warren, 1988). Essentially, most of the previous investigators solved the mass, momentum, and energy equations that describe laminar flow in a capillary or slit under conditions where viscous heating is important (Ybarra and Eckert, 1980; Dinh and Armstrong, 1982; Milthorpe and Tanner, 1987; Ko and Lodge, 1991). However, very few of them considered the combined effects of viscous heating and wall slip in numerical analysis. An attempt to do this was made by Lupton and Regester (1965). They carried out an analysis of the combined effects of slip velocity and viscous heating by using a simplified mathematical model for the flow of a power-law fluid, in an attempt to explain the origin of melt fracture.

In this study we present the results of a numerical simulation for the capillary flow of polymer melts in order to assess the effect of viscous heating on the slip-velocity measurements. Moreover, using our mathematical model, a new data analysis procedure is proposed that is found to be suitable for slip-velocity calculations corrected for the effect of viscous heating. The method is applied successfully to experimental data for several polymers, including polypropylene, high-density, and linear low-density polyethylenes.

The article is organized as follows. We begin our study with a presentation of the mathematical model. Then we discuss typical numerical results for a hypothetical material having properties similar to those of a typical polystyrene. We continue with a detailed description of the new capillary data-analysis technique, which can be used to decouple the slip velocity and viscous heating effects. Following this, we apply this data-analysis technique to interpret experimental data previously measured for polypropylene and linear-density polyethylene resins in our labs (Kazatchkov et al., 1995; Hatzikiriakos et al., 1995). Finally, we discuss the main results of this work and draw a few conclusions.

Mathematical Model

We consider the flow of a non-Newtonian fluid in a capillary of radius R and length L, with r and z as the coordinates in the radial and axial directions, respectively. The relevant nonzero velocity components are v_r and v_z, and the relevant physical properties of the fluid under consideration are its density ρ, heat capacity C_p, and thermal conductivity k. For our mathematical model we make the following assumptions:

- Steady laminar axisymmetric flow prevails.
- The radial velocity is sufficiently small to be neglected in the momentum and energy equations, and is included only in the continuity equation.
- Pressure variations in the radial direction are small compared to those in the axial direction.
- The effects of inertia and gravity are negligible.
- Axial heat conduction is negligible compared to axial convection.
- The heat capacity and thermal conductivity are considered to be temperature-dependent, and the fluid density is pressure- and temperature-dependent. The relevant equations to calculate these properties are from Van Krevelen (1992) and given in the Appendix.
- Fluid viscosity is a function of temperature and pressure, and the fluid follows a "power-law" model. The rz-component of the stress tensor may be written as follows:

$$\tau_{rz} = K \exp[\alpha P + A(T_{\text{ref}} - T)] \left| \frac{\partial v_z}{\partial r} \right|^{n-1} \left(\frac{\partial v_z}{\partial r} \right) \tag{1}$$

where τ_{rz} is the rz component of the stress tensor; P is the absolute pressure; T is the temperature; T_{ref} is a reference temperature; K and n are the consistency index and the power-law exponent of the power-law model; and α, and A, are the pressure- and temperature-dependent coefficients of the viscosity, respectively.

- There is a finite slip velocity at the wall u_s.

With these assumptions the equations of continuity momentum, and energy reduce to

$$\frac{1}{r}\frac{\partial(r\rho v_r)}{\partial r} + \frac{\partial(\rho v_z)}{\partial z} = 0 \tag{2}$$

$$\frac{\partial P}{\partial z} - \frac{1}{r}\frac{\partial(r\tau_{rz})}{\partial r} = 0 \tag{3}$$

$$\rho C_p v_z \frac{\partial T}{\partial z} = \frac{k}{r}\frac{\partial}{\partial r}\left(r\frac{\partial T}{\partial r} \right) + \tau_{rz}\left(\frac{\partial v_z}{\partial r} \right) + T\epsilon v_z \frac{dP}{dz}. \tag{4}$$

The mass flow-rate constancy equation is

$$2\pi \int_0^R \rho v_z r\, dr = m. \tag{5}$$

Boundary conditions: (6)

$$z = 0: \quad T = T_0$$

$$z = L: \quad P = 0$$

$$r = 0: \quad \partial T/\partial r = 0 \quad \partial v_z/\partial r = 0 \quad v_r = 0$$

$$r = R: \quad v_z = u_s \quad v_r = 0 \quad \frac{\partial T}{\partial r} = \frac{Bi}{R}(T_0 - T_W),$$

where Bi is the Biot number defined as

$$Bi = \frac{k_W}{k}\frac{1}{\ln(1 + t/R)},$$

where T_W, k_W, and t are the temperature, thermal conductivity, and thickness of the wall, respectively; T_0 = const is the temperature of the surroundings (at the outer surface of the die) taken to be equal to that of the polymer at the die inlet.

The second term on the right side of Eq. 4 is the viscous heating term, while the last term allows for the effect of expansion cooling due to fluid compressibility. The parameter ϵ is the coefficient of thermal expansion defined as $\epsilon = -(1/\rho)(\partial\rho/\partial T)_P$. Note that Eq. 4 is valid for both purely viscous and viscoelastic materials and independent of the choice of the constitutive equation (Astarita and Sarti, 1974).

The thermal boundary condition at the wall is not known in general, and one has to guess this condition. Most of the studies prescribe idealized conditions, such as:

- Constant wall temperature (T_W = const, $Bi \to \infty$);
- Adiabatic wall ($\partial T/\partial r = 0$, $Bi = 0$);
- Constant heat flux at the wall [$\partial T/\partial r$ = const, $Bi(T_0 - T_W)$ = const].

The latter condition was extensively and successfully used in numerous previous studies (e.g., Winter, 1977) and is believed to be the most realistic one. We will use only this thermal boundary condition in our numerical calculations.

For simplicity, the local slip Velocity is modeled at this point by a modified Power-law expression (no pressure and temperature dependence):

$$u_s = \frac{a}{1+(\sigma_c/\sigma_W)^{10}}\sigma_W^m, \tag{7}$$

where σ_W is the wall shear stress. The factor $1/[1+(\sigma_c/\sigma_W)^{10}]$ basically zeros the slip velocity for stresses less than σ_c and becomes about equal to one for shear stresses slightly greater than σ_c. It is noted that this model is only used to illustrate our method. A more general and accurate form of a slip velocity model will be presented and used below. Equations 1–8 were solved utilizing an implicit finite difference technique similar to that described by Warren (1988).

One final comment concerning thermal properties of the polymers is as follows. It is known that viscoelastic fluids are anisotropic and that their physical and thermal properties can exhibit a dependence on the history of the kinematics. Cocci and Picot (1973) reported a slight dependence of the effective thermal conductivity of polymers on the shear rate (up to 10% in the range of shear rates from 0 to 200 s^{-1}). The same effect can be expected for the heat capacity. However, there are no reliable expressions for considering these effects in our study. Nevertheless, we performed several test runs to estimate their influence on our calculations. We found that simultaneous increase of both thermal conductivity and heat capacity by 10% results in less than 1% change in the wall shear stress over a wide range of the shear rates. Based on this, the effect of deformation history on the thermal properties of polymers was excluded from our study.

Numerical Analysis and Results

To study the combined effect of viscous heating and wall slip, numerical simulations for the flow of a hypothetical polymer melt with physical properties similar to those of a typical polystyrene melt, were performed. These constants were found from Van Krevelen (1992) and are listed in Table 1. Three cases have been analyzed numerically in order to understand the relative significance of the viscous heating and

Table 1. Constants in Eqs. 1–8 for a Hypothetical Polystyrene Fluid

Eq. 1	A, K^{-1}	0.02
	K, Pa·s^n	35,000
	T_{ref}, °C	190
	α, Pa	3.5×10^{-9}
Eq. 8	n	0.4
	a	1.2
	σ_c, MPa	0.12
	m	3

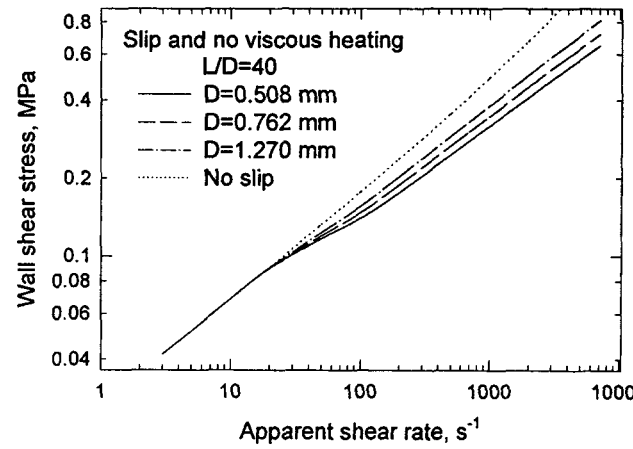

Figure 1. Calculated flow curves for a hypothetical material (physical properties listed in Table 1) under the influence of a slip boundary condition (slip with no viscous heating case).

slip flow effects on the flow curve (wall shear stress vs. apparent shear rate):

- No viscous heating with slip;
- Viscous heating with no slip;
- Viscous heating with slip.

First consider the case of *no viscous heating with slip*. Figure 1 plots the flow curves calculated for three capillary dies with different diameters, namely, 0.508, 0.762, and 1.27 mm, and a constant L/D ratio equal to 40. The quantities plotted in Figure 1 are defined as follows:

$$\dot{\gamma}_A = \frac{4Q}{\pi R^3} \tag{9}$$

$$\sigma_W = \frac{\Delta PR}{2L}, \tag{10}$$

where, $\dot{\gamma}_A$ is the apparent shear rate, ΔP is the total pressure drop along the capillary, and Q is the volumetric flow rate. It is noted that in the presence of viscous heating or for a pressure-dependent slip boundary condition, the wall shear stress is not constant along the capillary. Therefore, the previously defined wall shear stress only represents an average quantity.

It can be seen from Figure 1 that at some critical wall shear stress the curves start diverging, clearly indicating the diameter dependence of the flow curves. It can also be seen that the flow curve that corresponds to the capillary with the smaller diameter deviates more from the no-slip flow curve. These observations are consistent with the assumption of a wall-slip boundary condition and the applicability of the Mooney technique.

Now consider the second case, that is *viscous heating with no slip*. Figure 2 depicts flow curves for the same hypothetical polymer, capillary dies, and conditions as in the previous case (Figure 1). It can be seen that at relatively low values of the apparent shear rate all curves coincide, because the effect of viscous heating is insignificant at these small rates. However, as the apparent shear rate increases, the temperature increase becomes significant, and the flow curves start diverging and become diameter-dependent. The degree of diver-

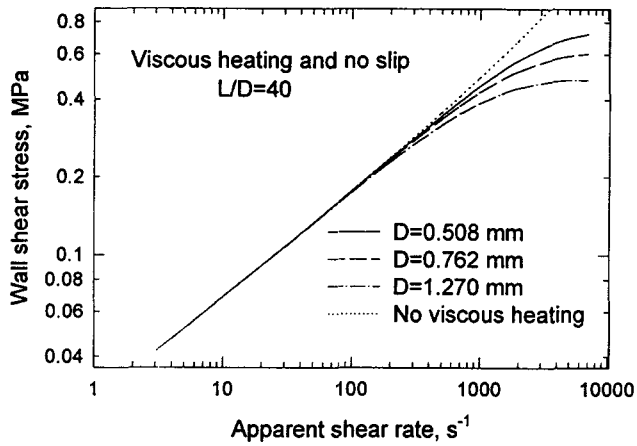

Figure 2. Calculated flow curves for a hypothetical material (physical properties listed in Table 1) under the influence of viscous heating effects (no slip with viscous heating case).

gence depends primarily on the physical properties of the polymer, and particularly on the temperature-dependent coefficient of the viscosity. However, the trend in the diameter dependence of the flow curves is opposite compared to that obtained in the first case (no viscous heating with slip). As can be seen from Figure 2, the viscous heating effect is more pronounced for capillary dies having a larger diameter. This is obvious since heat is conducted less efficiently radially in large dies. In addition, the die with the larger diameter is, in fact, longer since the ratio L/D is kept constant. Thus due to increased length the viscous heating is more significant for a capillary die of a larger diameter.

Obviously, it is reasonable to expect that in the presence of the two competing effects just described, namely those of slip and viscous heating on the flow curves, significant deviation from the assumptions of the Mooney method may result. Indeed, the case of *viscous heating with slip* is presented in Figure 3. The flow curves were calculated for the combined effect of wall slip and viscous heating for the same hypothetical material, capillary dies, and conditions. At the onset of slip

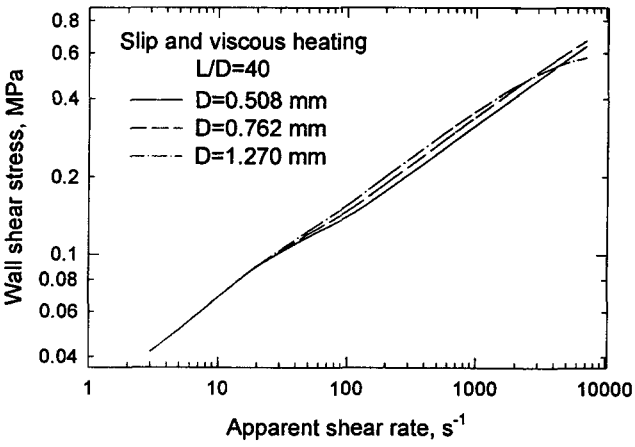

Figure 3. Calculated flow curves for a hypothetical material (physical properties listed in Table 1) under the influence of slip and viscous heating effects (slip with viscous heating case).

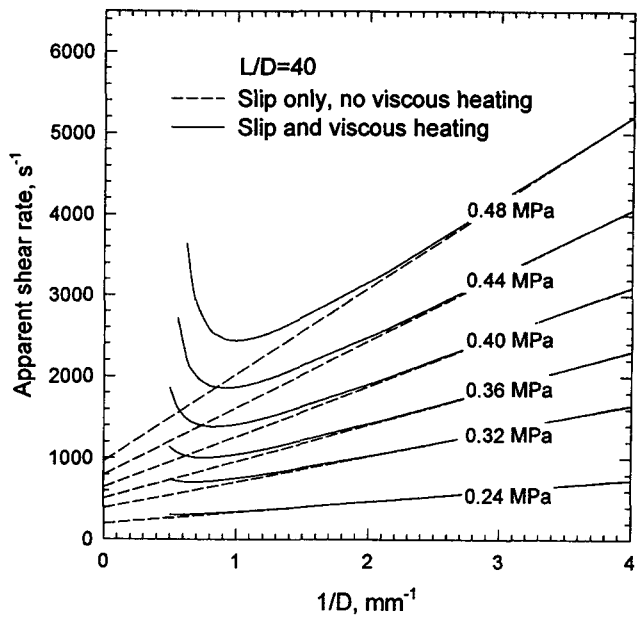

Figure 4. The effect of viscous heating on slip velocity measurements by means of Mooney plot.

flow, the curves start diverging, which indicates that slip occurs. At these relatively small apparent shear rates, the viscous heating effects are negligible and slip effects dominate. However, as the apparent shear rate increases, the effect of viscous heating becomes more significant, especially for capillary dies with a larger diameter. This effect causes significant deviation from the case of "no viscous heating with slip," and as a result at some point the flow curves converge, and cross each other at relatively higher apparent shear rates where the viscous heating effects become more dominant. Needless to say, for such a case the Mooney technique does not apply. It is also possible in some cases for the effect of viscous heating to mask the detection of wall slip by suppressing the diameter dependence of the flow curves. Such a case is discussed later.

To demonstrate the failure of the Mooney method in the presence of viscous heating effects, consider the Mooney plot in Figure 4, that is, the relationship between the apparent shear rate and the reciprocal capillary diameter at fixed values of the wall shear stress. Two cases have been plotted, those with and without viscous heating. One can see that consideration of viscous heating effects causes significant curvature to the Mooney plot particularly at higher shear stress values. Such curvature has been confirmed by many experimental studies (Lupton and Regester, 1965; Shih, 1979; Hatzikiriakos et al., 1995). This implies that some error in the calculation of the slip velocities using the Mooney technique is inevitable, especially in the case of significant viscous heating. Moreover, for capillary dies having a relatively large diameter, the thermal effects become quite substantial, especially at high wall shear stresses. As a result the curves pass through a minimum and turn upward sharply, as can be seen in Figure 4. These results are consistent with experimental data obtained by Vassalo (private communication) using an instrumented extruder and presented by Lupton and Regester (1965) (for example, see Figure 8 in their article).

Shidara and Denn (1993) carried out experiments with a polystyrene resin using a slit rheometer with the gaps ranging between 34 and 765 μm. These authors provided an explanation for their results that was found to be inconsistent with the Mooney technique. Their conclusion was that the observed effects were due to viscous heating. It should be pointed out that polystyrene, in general, has very high temperature- and pressure-dependent coefficients, and therefore viscous heating effects may be dominant. Based on the present numerical results, it is reasonable to believe that the combined effects of viscous heating and wall slip resulted in such a gap dependence of their data. In fact, their Figure 4 indicates a gap dependence that is opposite to what one expects to obtain in the presence of slip.

It is clear from the preceding numerical results that in cases where viscous heating is significant, data interpretation that only uses the Mooney technique is almost impossible, or if used may lead to large errors in calculating slip velocities. One way to alleviate this is by using only data obtained with capillaries that have small diameters. For such capillaries the effects of viscous heating are less significant. To see this more clearly, one can compare the slopes of the lines ($=8u_s$) in Figure 4 for the cases with and without viscous heating. The curves almost coincide for large values of $1/D$, that is, for small diameters. Unfortunately, capillaries having sufficiently small diameters to make the thermal effect negligible are not always available, or their use does not provide adequate information to completely characterize the flow behavior of a polymer. In addition, to obtain experimental data from such small-diameter capillaries is an extremely time-consuming procedure, and polymer degradation may become a factor due to the long pressure transients involved (Hatzikiriakos and Dealy, 1994).

Therefore at this point, it is desirable to use a mathematical method, which based on the experimental results, can calculate the true viscosity and slip velocity of the melts by accounting for the viscous heating effects. Essentially, this method should be able to solve the inverse problem, that is, given the experimental results estimate the slip velocity and rheological properties of the polymers (mainly viscosity) corrected for viscous heating effects. This is clearly an optimization problem. A procedure suitable for this purpose is described below.

Data Analysis Technique

To overcome the complications imposed by the viscous heating effects, the following procedure is proposed for analyzing capillary rheometry data.

- Capillary rheometry experiments are carried out using capillary dies having various diameters and L/D ratios (including orifice dies) and at different temperatures in order to assess the pressure, temperature, and end effects.
- Using the experimental data in the range of small apparent shear rates where the effects of wall slip and viscous heating are expected to be insignificant, the pressure dependence of viscosity can be determined.
- By applying the Rabinowitsch correction, the parameters of the power-law model, Eq. 1, and the temperature-dependent coefficient of viscosity can be calculated at small apparent shear rates.
- Using the entire set of experimental data, Eqs. 1–8 are solved in an iterative fashion to obtain the best fit of the calculated wall shear stress values to the experimental ones. To obtain this, the parameters of the slip-velocity model are used as variables. The average square deviation between predicted and measured values of the wall shear stress is used as a minimization criterion. The problem is subject to constraints on the parameters of the slip-velocity model. Thus any constrained optimization procedure can be used for this purpose. Instead of Eq. 8, any other appropriate form of the slip-velocity model can be chosen, depending on investigator's preferences.
- Using the optimal values of the slip-model parameters, the slip velocity is calculated for a given value of the wall shear stress. If the slip-velocity model used includes explicit pressure and temperature effects, the local slip velocity can be calculated by solving Eqs. 1–8, and the average slip velocity is determined as the mean slip velocity along the die. For an approximate but fairly accurate estimation, the slip velocity can be calculated directly from the slip model for a given temperature and wall shear stress.

The method of optimization employed in this study is the flexible tolerance method described in Himmelblau (1972). The method proved to be very reliable, though its execution time is fairly long. It provides only a local minimum, as do most local optimization methods. To determine a global minimum, several consecutive runs with different initial guesses should be carried out. The parameter estimates that provide the minimum value of the average square deviation are considered to be the global minimum.

Interpretation of Experimental Data

The procedure just described was tested on various polymers, namely high-density polyethylene (HDPE), linear low-density polyethylene (LLDPE), and polypropylene (PP). The case of HDPE (Sclair 56) is described in detail in Rosenbaum and Hatzikiriakos (1996). It is found that viscous heating is not significant for this resin, and the modified Mooney technique employed by Hatzikiriakos and Dealy (1992) results in fairly accurate estimates of the slip velocity. Below we examine the capillary flow of polypropylene and linear low-density polyethylene in order to assess the relative importance of slip and viscous heating effects.

Combined slip and viscous heating effects in the capillary flow of a PP resin

The second system examined within the context of the proposed procedure was that studied by Kazatchkov et al. (1995). The polymer used in that study was polypropylene (PP), which has a molecular weight M_W of 762,000. Experiments were carried out on an Instron constant-speed piston-driven capillary rheometer using circular dies of various diameters and L/D ratios. Flow curves obtained for this resin using capillary dies of different diameters and constant $L/D = 40$ are presented in Figure 5.

As can be seen from Figure 5, these flow curves show no divergence, implying the absence of slip, at least in terms of the Mooney technique. However, in that study the authors concluded that slip is present, though its determination by the Mooney technique is impossible due to the fact that strong

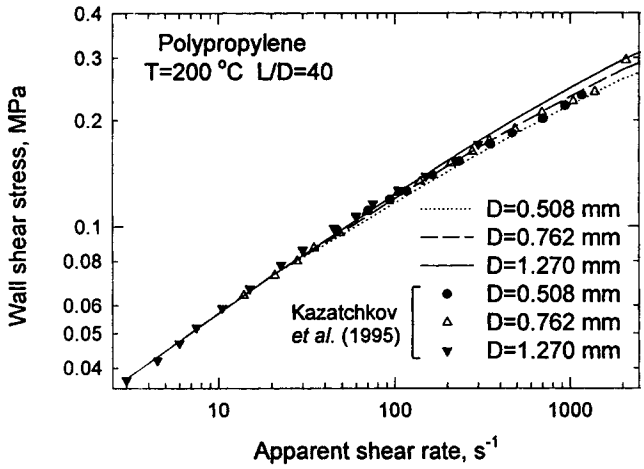

Figure 5. Experimental and calculated flow curves for a polypropylene resin for three capillary dies having the same *L/D* ratio of 40 and various diameters.

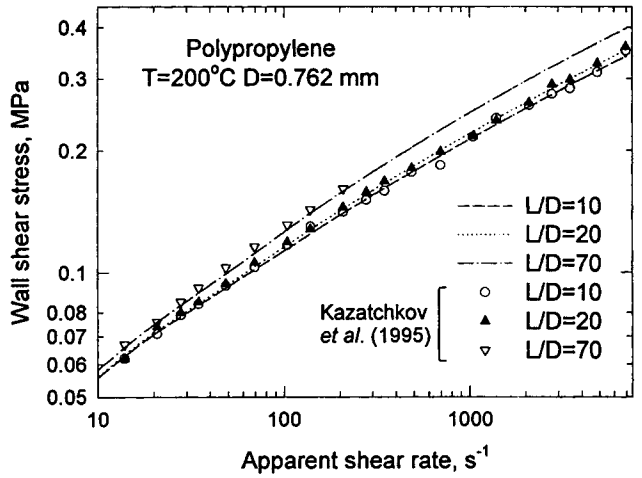

Figure 6. Experimental and calculated flow curves for a polypropylene resin for three capillary dies having the same diameter and various *L/D* ratios.

viscous heating effects mask the diameter dependence of the flow curves. This conclusion was drawn on the basis of the following observations: PP extrudates appear to be distorted for apparent shear rates beyond a certain value. These visual defects on the surface of extrudates are always accompanied by wall slip for other systems such as high-density and linear low-density polyethylenes (Ramamurthy, 1986; Kalika and Denn, 1987; Hatzikiriakos and Dealy, 1992). Thus, the authors believed that this should also be the case for PP. Furthermore, application of the time–temperature superposition principle to superpose viscosity data failed for apparent shear rates beyond a certain value, which was found to be the same as that for the appearance of surface defects. In addition, viscosity data at higher temperatures were found to deviate more from power-law behavior, mainly because slip velocity increases with temperature.

One can also confirm that the effect of viscous heating is more significant for the case of PP compared to those of HDPE and LLDPE by examining the flow-activation energies, E^*, using an Arrhenius type of equation to model the temperature dependence of viscosity $\eta = A\exp(E^*/RT)$ (Van Krevelen, 1992; Wang and Porter, 1995). For PP it is about 10 kcal/mole, for LLDPE, about 6.3 kcal/mole, and much less for HDPE. On the other hand, PS (the hypothetical material examined in Figures 1–4) has a very high value for E^*, close to 20 kcal/mole, which implies that viscous effects are even more dominant in the capillary flow of this resin.

Another way to conclude that viscous heating plays a significant role in the flow of PP is to calculate the Nahme number that compares the relative effect of temperature changes due to viscous heat generation to those due to heat conduction in the radial direction. This dimensionless number is defined as $Na = A\bar{v}^2\bar{\eta}/\bar{k}$ (Winter, 1977), where A is the temperature-dependent coefficient in Eq. 1, $\bar{v}$ is the mean axial velocity, $\bar{k}$ is the mean thermal conductivity at the reference temperature, and $\bar{\eta}$ is the reference viscosity corresponding to a reference shear rate $\bar{\dot{\gamma}} = \bar{v}/R$. For the apparent shear rate of 1,000 s^{-1} the mean velocity in the capillary of $R =$ 0.635 mm is 0.16 m/s, the thermal conductivity at 200°C is 0.12 W/(m·K), $\bar{\dot{\gamma}} = 250\ s^{-1}$, and $\bar{\eta} \approx 500$ Pa·s. The Nahme number is 1.07 for these conditions of the flow of PP, which is greater than $0.1 \div 0.5$, thus indicating that viscous dissipation leads to significant viscosity changes, that is, changes reflected in the temperature and velocity fields.

To check the validity of this conclusion, the proposed data-analysis technique was used to calculate the slip velocity in the flow of molten polypropylene using the experimental data shown in Figures 5 and 6. Figure 5 plots flow curves of PP obtained by using capillaries with a constant length-to-diameter ratio, $L/D = 40$, and different diameters, and Figure 6 plots flow curves of PP obtained by using capillaries with a constant diameter and various length-to-diameter ratios, L/D.

The local slip velocity was modeled by using the modified power-law expression proposed by Hatzikiriakos and Dealy (1992). This can be written as

$$u_s = \frac{\xi_0 f_1(T)}{1+(\sigma_c/\sigma_w)^{100}}\left(1 - c_1 \tanh\frac{E + c_2\sigma_n/\sigma_w}{RT}\right)\left(\frac{\sigma_w}{\sigma_c I^{1/4}}\right)^m, \tag{11}$$

where ξ_0, c_1, c_2, and m are coefficients; $f_1(T)$ is a function of temperature (the WLF equation, $f_1(T) = C_1(T - T_0)/[C_2 + (T - T_0)]$, where C_1 and C_2 are constants, is used); E is an activation energy for adsorption/desorption; σ_w is the local wall shear stress; σ_n is the local normal stress at the wall; σ_c is the critical shear stress for the onset of slip; and I is the resin polydispersity. Note that the denominator $1+(\sigma_c/\sigma_w)^{100}$ must be included in order to zero the slip velocity for wall shear stresses less than the critical value, σ_c. The normal stress can be approximated by (Hatzikiriakos and Dealy, 1992)

$$\sigma_n = P + 50\sigma_w/12. \tag{12}$$

Note that the slip model Eq. 11 takes into account both the temperature and pressure dependence of the slip velocity.

Table 2. Constants for PP and LLDPE

		PP	LLDPE
Polydispersity	I	1	3.9
Thermal conductivity of the wall	k_W, W/(m·K)	17.0	17.0
Eq. 1	A, K^{-1}	0.01	0.0075
	K, Pa·s^n	21,956	8,100
	T_{ref}, °C	200	200
	α, Pa	5.9×10^{-9}	4×10^{-9}
	n	0.34337	0.674
WFL equation	C_1	1.159	2.552
	C_2, K	109.43	83.61

The values of the parameters for Eqs. 1 and 11 are given in Table 2 along with other physical properties of polypropylene. The constant heat-flux thermal boundary condition was used in the numerical simulations. The optimization program includes as constraints that (1) the adjustable parameters ξ_0, c_1, c_2, m, E, and σ_c be positive, and (2) the slip velocity should not exceed the average velocity obtained from a plug-flow assumption. The number of experimental points was 43. The optimal values of the slip velocity model parameters are listed in Table 3. The calculations were repeated several times, each time starting with a different initial guess, and the program always recovered the same set of values. These values are believed to provide a unique solution to the problem and to be a global minimum as well. The average deviation from the experimental data was about 2.9%.

The calculated flow curves for the dies with diameters of 0.508 mm, 0.762 mm, and 1.27 mm and the same L/D ratio of 40 are presented in Figure 5, along with the experimental data points. One can see the excellent agreement between experimental and simulated data. In particular, the flow curves seem to almost coincide, implying the absence of wall slip (no diameter dependence). As discussed and presented below, however, our calculations have shown that slip does occur. Figure 6 shows fitted and experimental flow curves obtained for the capillaries of the same diameter and various L/D ratios that are again in very good agreement. Divergence between the flow curves indicates that the viscosity is a function of pressure.

Figure 7 depicts predicted slip velocity, wall shear stress, pressure and temperature rise profiles (axial) for capillary dies with the same diameter, and various L/D ratios. The average wall shear stress is 0.3 MPa for all dies. However, it can be seen that the actual wall shear stress profiles vary with changes in the L/D ratio. For a short capillary the shear stress is almost a linear function of the axial position, decreasing gradually throughout the length of the capillary. However, in a long die the shape of the curve becomes slightly convex upward and the wall shear stress decreases significantly along the length of the die. The pressure drop is almost linear along the die. The slip velocity is strongly affected by the combination of these parameters, σ_W, T, and P. In short capillaries where the temperature rise is small enough, it is nearly constant along the die. As the L/D ratio increases, the pressure becomes a factor and the average slip velocity decreases. However, since the effect of viscous heating is more pronounced for longer capillaries, the slip velocity is not constant throughout the die anymore, thus decreasing with increases in the temperature. The dip in the slip-velocity profile becomes larger and deeper as the L/D ratio increases. At the die exit the reduction of pressure causes the slip velocity to increase, thus diminishing the effect of temperature.

Figure 8 presents the predicted slip velocity, wall shear stress, pressure, and temperature-rise profiles (axial) for capillaries with $L/D = 40$ and different diameters. The same trend can be observed in this case; that is, the slip velocity first decreases due to viscous heating, then passes through a minimum, and increases close to the die exit as a result of pressure reduction. The curvature of the slip-velocity profile depends on the temperature rise, which is greater for capillaries with larger diameters.

The average temperature rises plotted in Figures 7 and 8 are, in general, more pronounced for longer dies that have the same diameter and for larger dies with a constant L/D ratio. In a long die the residence time of the melt is higher, and thus the melt is subject to larger amounts of heat-dissipation. However, for long enough capillaries this trend may be reversed because expansion cooling becomes significant. Indeed, it can be seen in Figure 7 that the average temperature rise is higher in the capillary with an $L/D = 40$ than in the capillary with an $L/D = 70$. While energy dissipation is higher for the $L/D = 70$, expansion cooling reduces the temperature in the core region of the melt significantly, with the result that the average temperature rise is kept small. In general, it can be seen in Figures 7 and 8 that the calculated

Table 3. Calculated Parameters of the Slip Velocity Model, Eqs. 11 and 13

	Polypropylene		Polyethylene	
Parameter	Equation 11	Equation 13	Equation 11	Equation 13
ξ_0, m/s	0.8219×10^{-2}	0.8219×10^{-2}	0.1227×10^{-1}	0.1227×10^{-1}
c_1	0.968	0.968	0.988	0.988
c_2, cal/mol	7.19	14.38	15.27	30.54
E, cal/mol	1,422.6	1,452.6	1,203.0	1,266.6
σ_c, Pa	0.911×10^5	0.911×10^5	0.807×10^5	0.807×10^5
m	4.897	4.897	4.312	4.312

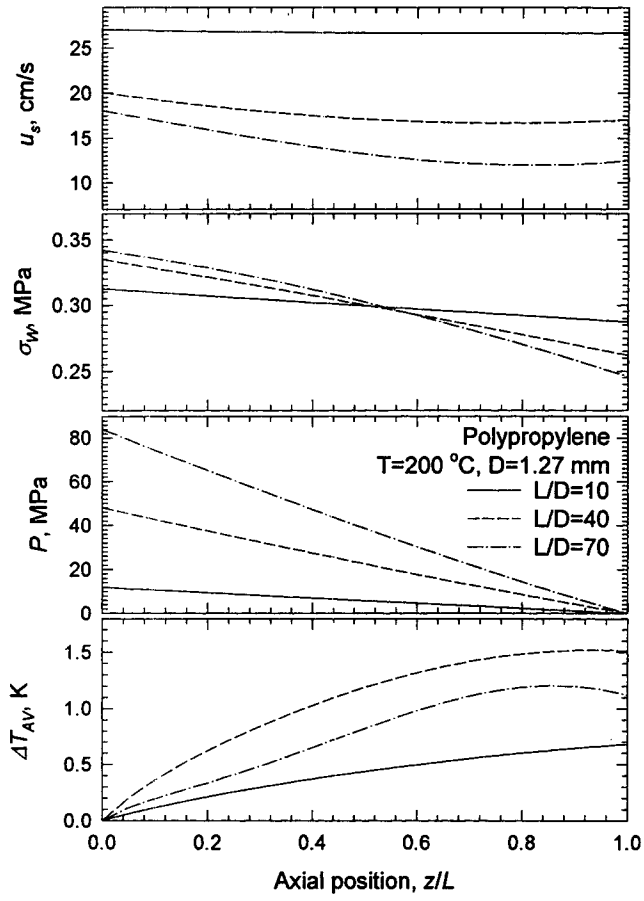

Figure 7. Calculated axial slip velocity, wall shear stress, pressure, and average temperature rise in the capillary flow of a polypropylene resin for three dies having the same diameter and various *L/D* ratios.

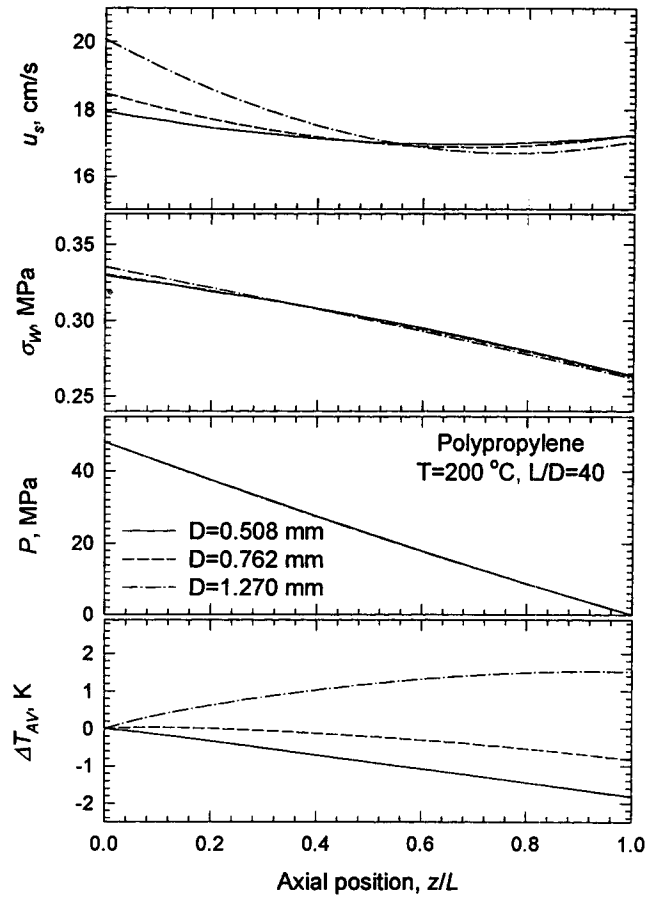

Figure 8. Calculated axial slip velocity, wall shear stress, pressure, and average temperature rise in the capillary flow of a polypropylene resin for three dies having the same *L/D* ratio and various diameters.

average temperature rises are small, so one would expect that viscous heating is not significant. However, the maximal temperature rise close to the wall may exceed the average one by several times reaching quite significant values. It is this temperature rise that significantly influences the rheological measurements and always increases with L/D (D = const) and D (L/D = const). Figure 9 plots the radial temperature profiles at the die outlet for the two cases described in Figures 7 and 8. We can see that the higher temperature rise occurs in the region close to the wall. This is the region of high shear, and thus that of the largest temperature rise. At the same time, this is the region where temperature has the strongest influence on the rheological measurements as well as the slip-velocity ones. In the core region of the die, however, expansion cooling is dominant, thus causing the temperature to drop significantly. Expansion cooling caused by the small but finite polymer compressibility is strongly affected by the pressure; hence, it is more pronounced for the capillaries with larger L/D ratios.

From the slip-velocity model used and the numerical results presented in Figures 7 and 8, it is obvious that the slip velocity is a function of the wall shear stress, wall normal stress, and temperature; thus, it varies with the axial position along the die. However, it is often desirable to find the average slip velocity as a function of the average wall shear stress for capillaries with various length-to-diameter ratios. This can be done by first assuming that pressure changes linearly in a capillary (a good approximation). Second, we can express the normal stress σ_n, in terms of L/D, and substitute the results in Eqs. 11–12 (for more details, see Hatzikiriakos and Dealy, 1992). We can obtain the following expression for the slip velocity:

$$u_s = \frac{\xi_0 f_1(T)}{1+(\sigma_c/\sigma_W)^{100}}\left(1-c_1\tanh\frac{E^*+c_2^*L/D}{RT}\right)\left(\frac{\sigma_W}{\sigma_c I^{1/4}}\right)^m, \tag{13}$$

where $E^* = E + 50c_2/12$, and $c_2^* = 2c_2$. The significance of this equation is that the obtained slip-velocity values can now be compared directly with the experimentally determined ones. Figure 10 plots the slip velocity of PP as a function of wall shear stress for various L/D capillary ratios. The optimum values of the parameters in Eqs. 11 and 13 calculated from the minimization algorithm, are listed in Table 3. As

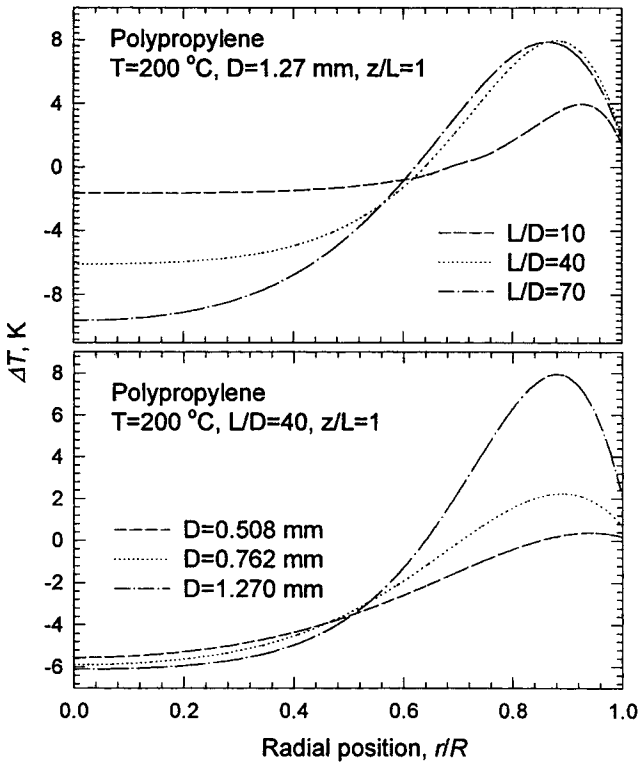

Figure 9. Calculated radial temperature profiles at the die outlet in the capillary flow of a polypropylene resin for dies having various *L/D* ratios and diameters.

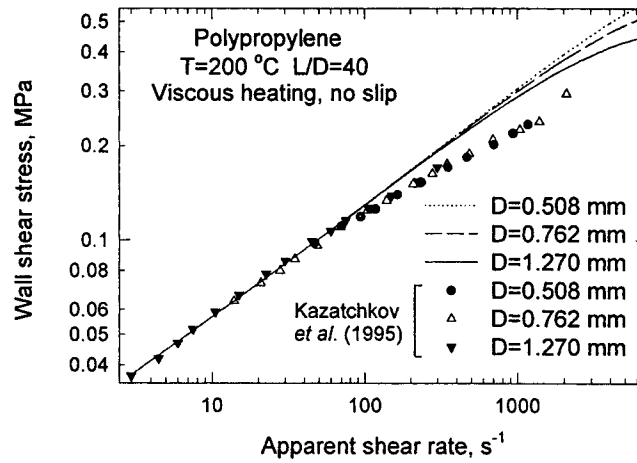

Figure 11. Experimental flow curves and those calculated in the absence of wall slip for a polypropylene resin for three capillary dies having the same *L/D* ratio of 40 and various diameters.

can be seen in Figure 10, despite the apparent absence of slip from the experimental data of Figure 5, the slip velocity of PP is considerable. At high enough shear stresses, it exceeds that calculated for a HDPE (Hatzikiriakos and Dealy, 1992). In addition, the calculated slip velocities scale with *L/D* ratio, indicating the same trend as that observed experimentally.

Figure 11 compares the experimental results presented in Figure 5 with the model predictions in the absence of wall slip. It is clear that viscous heating is significant due to the presence of diameter dependence, and the overall description of the data in the absence of wall slip becomes poor. Thus, the inclusion of wall slip is a necessary ingredient of our model in adequately describing the capillary flow of PP at high enough shear rates where the effects of viscous heating and wall slip become significant.

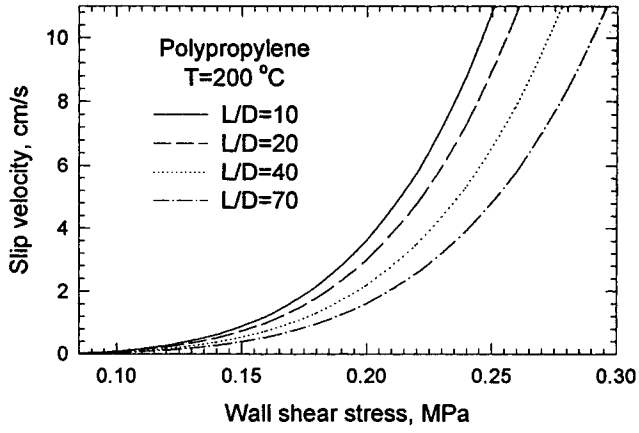

Figure 10. Calculated slip velocity of a polypropylene resin as a function of wall shear stress for capillary dies having various *L/D* ratios.

Combined slip and viscous heating effects in the capillary flow of an LLDPE resin

The case of PP demonstrated an example of how the slip velocity of a polymer can be calculated when macroscopic experimental data imply the absence of slip (no diameter dependence of flow curves). For such a case the Mooney method is obviously not applicable. However, it would be interesting to examine one case where capillary data were actually used to determine the slip velocity. For such a case, using our mathematical model, it would be possible to estimate the error resulting from the curvature of the lines in the Mooney plot.

To answer this question, the experimental data for a linear low-density polyethylene (LLDPE, Dowlex 2049) reported by Hatzikiriakos et al. (1995) are used to calculate the parameters of the slip-velocity model for this polymer (Eq. 11). The authors reported that the Mooney plots were severely curved and identified this as a viscous heating effect. In spite of this, straight lines were fitted to the data, and thus the slip velocity was calculated as a function of the wall shear stress for a number of capillaries with various *L/D* ratios.

The values of the parameters used in Eqs. 1 and 11 are tabulated in Table 2. The number of experimental points was 46. The optimal values of the slip-velocity model parameters calculated by the optimization technique are listed in Table 3. The average deviation from the experimental data was about 5.9%. Figure 12 shows experimental and predicted flow curves for capillaries that have the same *L/D* ratio and different diameters. As can be seen, the obtained deviation

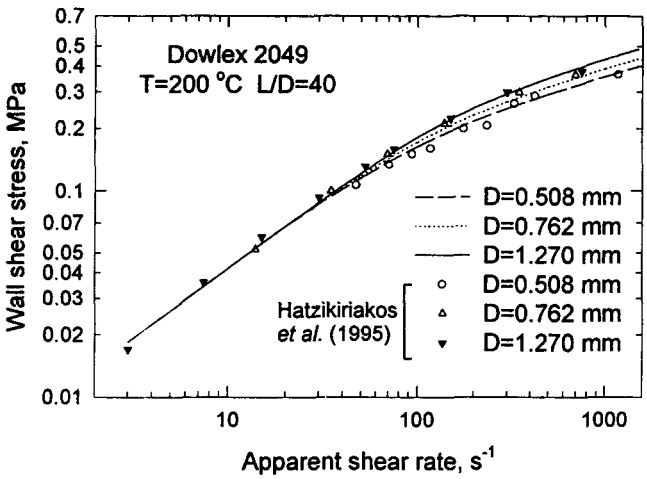

Figure 12. Experimental and calculated flow curves for a linear low-density resin (Dowlex 2049) for three capillary dies having the same *L/D* ratio of 40 and various diameters.

(5.9%) can be attributed to experimental error and primarily comes from fitting the data corresponding to the capillary die with the smallest diameter.

Figure 13 compares the slip velocities calculated with Eq. 13 using the values of the parameters listed in Table 3, with those calculated from macroscopic experimental data reported by Hatzikiriakos et al. (1995). One can identify quite significant differences between the slip-velocity values predicted by the present procedure (continuous lines) and those calculated using the graphical Mooney technique (symbols). These differences become more significant at relatively high wall shear stress values (viscous heating effects dominate). The agreement between the predicted values and the experimental data obtained for the special case of $L/D = 0$ is remarkably good. These data correspond to the slip velocity

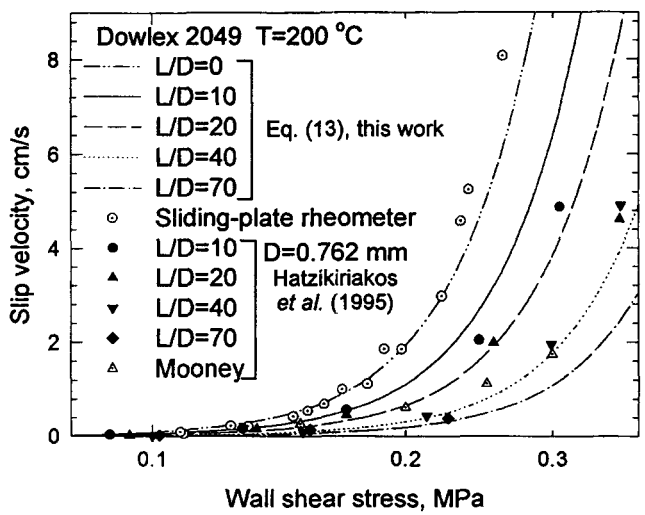

Figure 13. Experimental and calculated slip velocities of a linear low-density resin (Dowlex 2049) as a function of wall shear stress for capillary dies having various *L/D* ratios.

obtained from a sliding plate rheometer operated at ambient pressure. This is due to the fact that viscous heating effects are negligible in a sliding-plate rheometer compared to those in a capillary rheometer (Dealy, 1982). It should be noted that the sliding-plate rheometer data were not used in the fitting procedure. They were estimated by using the calculated values of the model parameters. In addition, Figure 13 shows that the disagreement between the slip-velocity predictions and the capillary rheometer data increases with increase in *L/D*, that is, with increase in the significance of the viscous heating effects.

Conclusions

The problem of evaluating the slip velocity in the capillary flow of molten polymers based on experimental results (for example, diameter dependence of flow curves) was studied in detail. It was found that in cases where viscous heating effects are significant, the traditional methods used to estimate the slip velocity (for example, Mooney's technique) often fail to give accurate or even physically meaningful results. In the present work, a data-analysis procedure based on a mathematical model for the nonisothermal capillary flow of polymer melts coupled with heat transfer is developed.

The computer simulations proposed can be used for two purposes: to provide detailed velocity, temperature, and pressure distributions that can be useful in designing dies; and to recover the parameters of the slip-velocity model used, corrected for the effect of viscous heating. The method was used to correct experimental capillary results obtained for various polymers, including PP, high- and low-density PE. It was found that the results corrected for viscous heating effects are consistent with experimental data.

Acknowledgments

This work was financially supported from a grant provided by the Natural Sciences and Engineering Research Council of Canada.

Literature Cited

Astarita, G., and G. C. Sarti, "Thermomechanics of Compressible Materials with Entropic Elasticity," *Theoretical Rheology*, Wiley, New York, p. 123 (1974).

Blyler, L. L. and A. C. Hart, "Capillary Flow Instability of Ethylene Polymer Melts," *Polym. Eng. Sci.*, **10**, 193 (1970).

Cocci, A. A., and J. J. C. Picot, "Rate of Strain Effect on the Thermal Conductivity of a Polymer Liquid," *Polym. Eng. Sci.*, **13**, 337 (1973).

Cox, H. W., and C. W. Macosko, "Viscous Dissipation in Die Flows," *AIChE J.*, **20**(4), 785 (1974).

Dealy, J. M., *Rheometers for Molten Plastics*, Van Nostrand, New York, p. 60 (1982).

Dinh, S. M., and R. C. Armstrong, "Non-isothermal Channel Flow of Non-Newtonian Fluids with Viscous Heating," *AIChE J.*, **28**(2), 294 (1982).

Hatzikiriakos, S. G., and J. M. Dealy, "Wall Slip of Molten High Density Polyethylene. I. Sliding Plate Rheometer Studies," *J. Rheol.*, **35**(4), 497 (1991).

Hatzikiriakos, S. G., and J. M. Dealy, "Wall Slip of Molten High Density Polyethylene. II. Capillary Rheometer Studies," *J. Rheol.*, **36**(4), 703 (1992).

Hatzikiriakos, S. G., and J. M. Dealy, "Start-up Pressure Transient in a Capillary Rheometer," *Polym. Eng. Sci.*, **34**(6), 493 (1994).

Hatzikiriakos, S. G., P. Hong, W. Ho, and C. W. Stewart, "The Effect of Teflon Coatings in Polyethylene Capillary Extrusion," *J. Appl. Polym. Sci.*, **55**, 595 (1995).

Table A1. Constants for the Three Resins Studied: Polyethylene, Polypropylene, Polystyrene

Type of Polymer	π, bar	ω, cm^3/g	M, g/mol	C_p^{298}, J/(mol·K)	T_g, K	$k(T_g)$, W/(m·K)
Polypropylene	2,470	0.83	42.1	91	260	0.144
Polyethylene	3,290	0.88	28.1	63	195	0.326
Polystyrene	1,870	0.82	104.1	178	373	0.172

Himmelblau, D. M., *Applied Nonlinear Programming*, McGraw-Hill, New York, p. 498 (1972).

Kalika, D. S., and M. M. Denn, "Wall Slip and Extrudate Distortion in Linear Low-Density Polyethylene," *J. Rheol.*, **31**(8), 815 (1987).

Kazatchkov, I. B., S. G. Hatzikiriakos, and C. W. Stewart, "Extrudate Distortion in the Capillary/Slit Extrusion of a Molten Polypropylene," *Polym. Eng. Sci.*, **35**(23), 1864 (1995).

Ko, Y. S., and A. S. Lodge, "Viscous Heating Correction for Thermally Developing Flows in Slit Die Viscometry," *Rheol. Acta*, **30**, 357 (1991).

Lupton, J. M., and R. W. Regester, "Melt Flow of Polyethylene at High Rates," *Polym. Eng. Sci.*, **5**, 235 (1965).

Milthorpe, J. F., and R. I. Tanner, "On the Extrusion of Visco-elastic Fluids Subject to Viscous Heating," *Int. J. Numer. Methods Eng.*, **24**, 263 (1987).

Mooney, M., "Explicit Formulas for Slip and Fluidity," *J. Rheol.*, **2**, 210 (1931).

Ramamurthy, A. V., "Wall Slip in Viscous Fluids and Influence of Materials of Construction," *J. Rheol.*, **30**(2), 337 (1986).

Rosenbaum, E. E., and S. G. Hatzikiriakos, "The Effect of Viscous Heating in Capillary Rheometry," SPE ANTEC '96 Tech. Papers, **42**, 1080–1084 (1996).

Shidara, H., and M. M. Denn, "Polymer Melt Flow in Very Thin Slits," *J. Non-Newtonian Fluid Mech.*, **48**, 101 (1993).

Shih, C.-K., "Capillary Extrusion and Mold Flow Characteristics of an Incompatible Blend of Two Elastomers," *Science and Technology of Polymer Processing*, MIT Press, Cambridge, MA, p. 528 (1979).

Van Krevelen, D. W., *Properties of Polymers: Their Correlation with Chemical Structure; Their Numerical Estimation, and Prediction from Additive Group Contributions*, Elsevier, New York (1992).

Wang, J., and R. S. Porter, "On the Viscosity-Temperature Behavior of Polymer Melts," *Rheol. Acta*, **34**, 496 (1995).

Warren, R. C., "Viscous Heating," *Rheological Measurement*, Elsevier, London, p. 119 (1988).

Winter, H. H., "Viscous Dissipation in Shear Flows of Molten Polymers," *Adv. Heat Transfer*, **13**, 205 (1977).

Ybarra, R. M., and R. E. Eckert, "Viscous Heat Generation in Slit Flow," *AIChE J.*, **26**(5), 751 (1980).

Appendix: Relationships to Calculate Physical Properties of the Polymers Studied

All correlations, relationships, and physical properties are taken from Van Krevelen (1992). The density of polymers is assumed to be a function of temperature and pressure, that is, $\rho = \rho(T,p)$ (Table A1). It is modeled by using the Spencer–Gilmore equation (modified van der Waals equation), which has the following form:

$$(1/\rho - \omega)(p + \pi) = RT/M, \tag{A1}$$

where ρ is density (g/cm^3); p is applied pressure (bar); T is temperature (K); ω is specific volume at $p = 0$ and $T = 0$ (cm^3/g); π is internal pressure (bar); and M is the molecular mass of the interacting unit, which is usually identical to the structural unit of the polymer (g/mol). From Eq. A1 one can calculate the density as

$$\rho = \left(\frac{RT}{M(p + \pi)} + \omega \right)^{-1}. \tag{A2}$$

The coefficient of thermal expansion is defined as: $\epsilon \equiv -(1/\rho)(\partial\rho/\partial T)_p$.

The term ϵT in the energy equation (Eq. 4) can be obtained by differentiating Eq. A2 with respect to T:

$$\epsilon T = 1 - \rho\omega. \tag{A3}$$

The heat capacity is assumed to be a function of temperature and is given by

$$C_p(T) = C_p(298)\cdot(1 + 1.2\cdot10^{-3}\cdot T), \tag{A4}$$

where C_p is in J/(mol·K), T in °C.

The thermal conductivity is assumed to be a function of temperature. From a generalized curve for the thermal conductivity of polymers (Van Krevelen, 1992), one can find for $T > T_g$

$$k(T) = k(T_g)\cdot(1.2 - 0.2\cdot T/T_g), \tag{A5}$$

where T_g is the glass transition temperature (K), and $k(T)$ is in W/(m·K).

Manuscript received Mar. 7, 1996, and revision received Sept. 25, 1996.